Supplementary material

This document provides supplementary material supporting the paper "Observation of long-range elliptic azimuthal anisotropies in $\sqrt{s}$ =13 and 2.76 TeV pp collisions with the ATLAS detector".

Figure 1 shows the template fits to the $Y(\Delta\phi)$ in 13 TeV pp collisions for charged particle pairs having $0.5 < p_{\mathrm{T}}^{\mathrm{a,b}} < 5$ GeV and $2 < |\Delta\eta| < 5$. Each panel represents a different $N_{\mathrm{ch}}^{\mathrm{rec}}$ interval. The open points indicate $FY^{\mathrm{periph}}(\Delta\phi) + G$, while the solid and dashed curves show the full template functions and $Y^{\mathrm{ridge}}(\Delta\phi) + FY^{\mathrm{periph}}(0)$, respectively. The horizontal short-dashed line indicates $G + FY^{\mathrm{periph}}(0)$. Similar fits for the 2.76 TeV data are shown in Fig. 2. In every multiplicity interval, the template fit well describes the data. The quality of the fits leaves no room for significant modification of the peak at $\Delta\phi = \pi$ except for that resulting from the sinusoidal term.

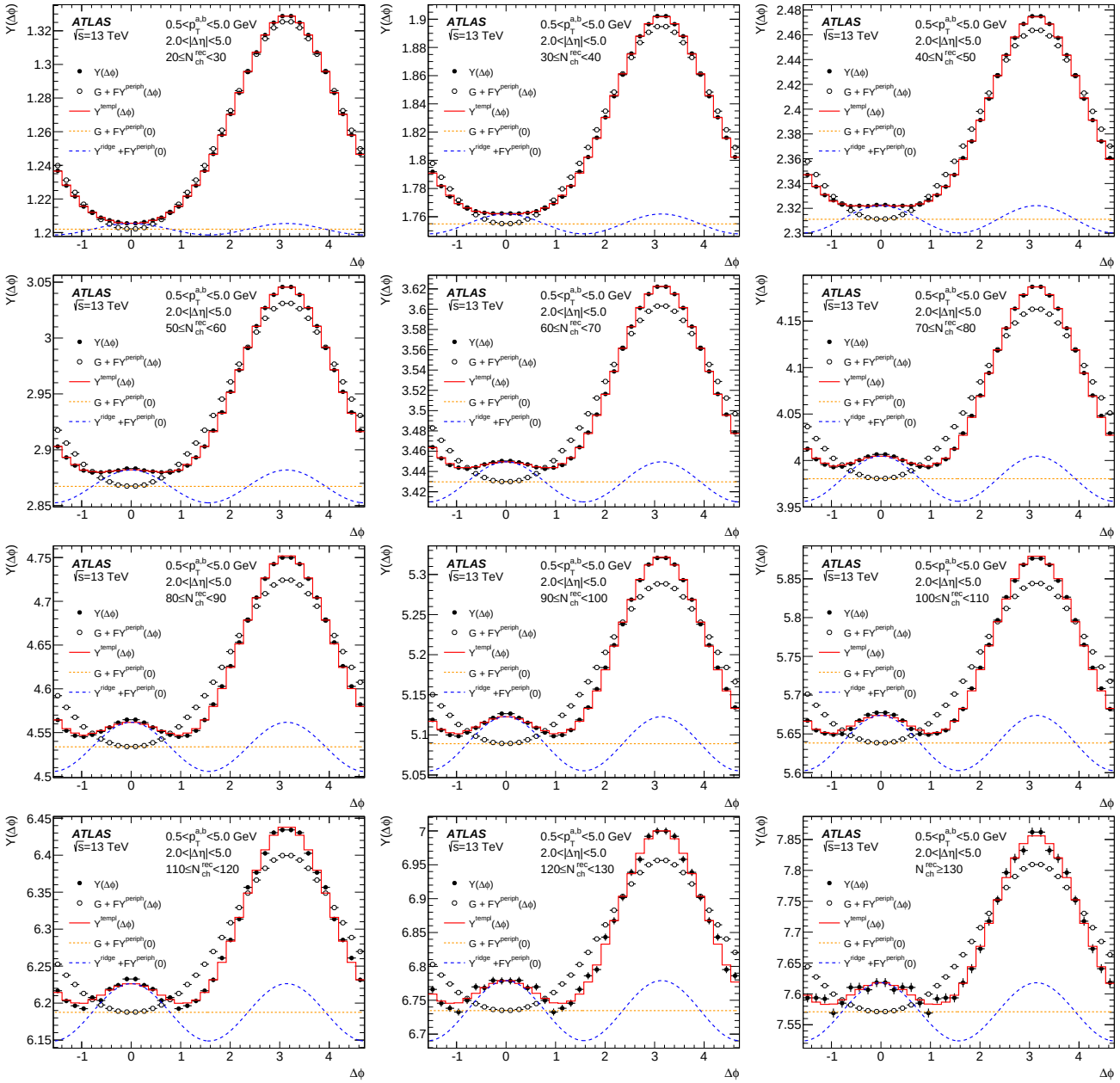

Figure 1: Template fits for all of the analyzed multiplicity intervals in the 13 TeV data for $0.5 < p_{\mathrm{T}}^{\mathrm{a,b}} < 5$ GeV. The open points and curves show different components of the template (see legend) that are shifted, where necessary, for presentation. Each panel is a different multiplicity bin. The vertical error bars on the data-points indicate statistical uncertainties.

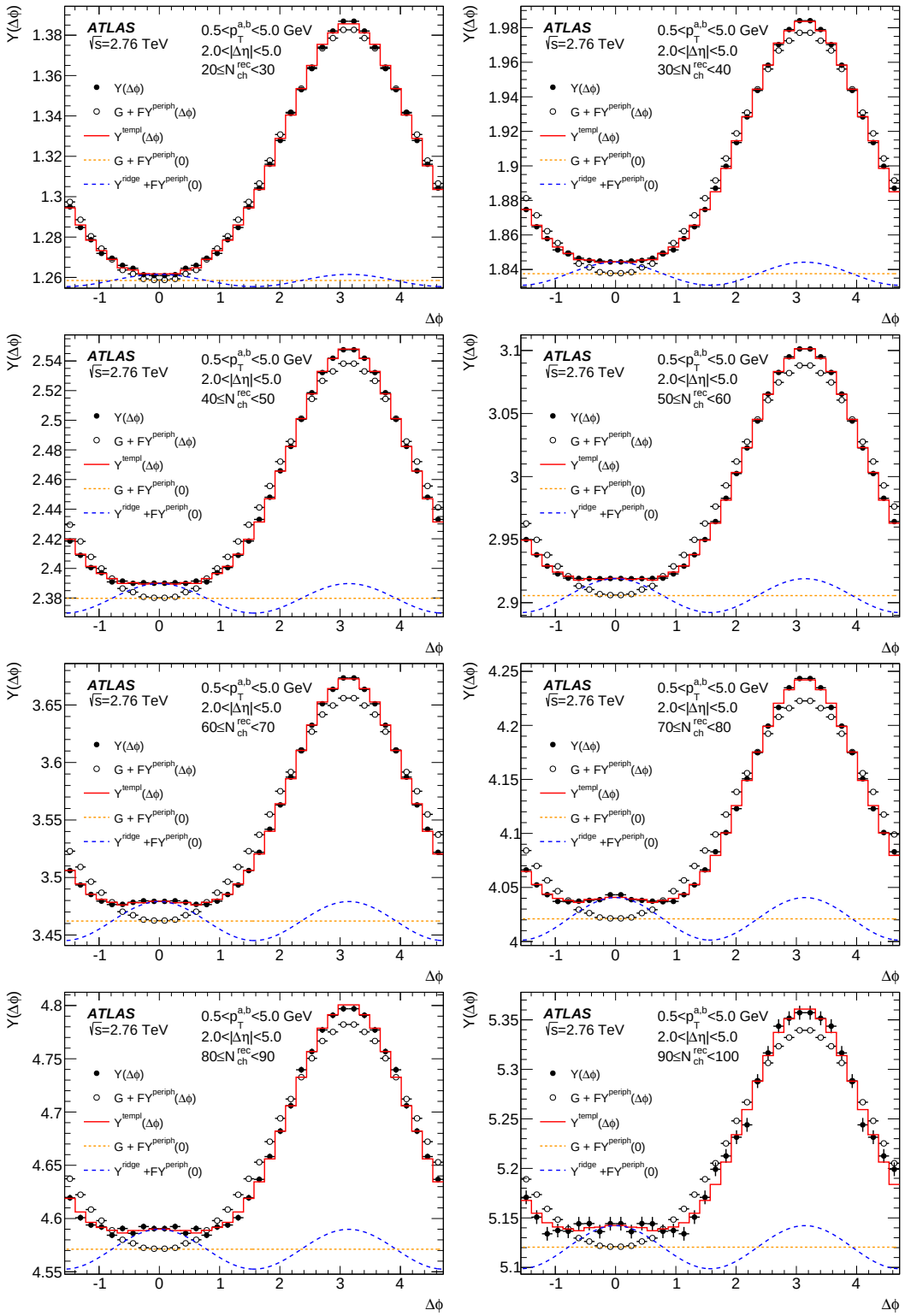

Figure 2: Template fits for all of the analyzed multiplicity intervals in the 2.76 TeV data for $0.5<p_{\mathrm{T}}^{\mathrm{a,b}}<5$ GeV. The open points and curves show different components of the template (see legend) that are shifted, where necessary, for presentation. Each panel is a different multiplicity bin. The vertical error bars on the data-points indicate statistical uncertainties.

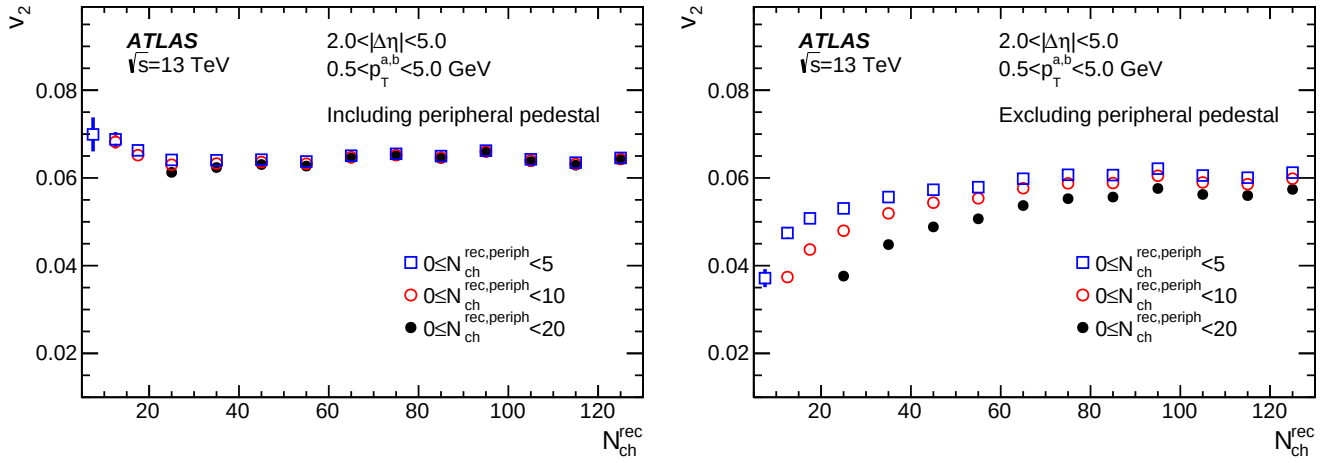

Figure 3: Left panel: the $N_{\rm ch}^{\rm rec}$ dependence of v_2 in 13 TeV data for $0.5<p_{\rm T}<5$ GeV for three different choices of the peripheral multiplicity interval, $N_{\rm ch}^{\rm rec,periph}$. Right panel: similar plot but with the pedestal, $Y^{\rm periph}(0)$, subtracted from $Y^{\rm periph}(\Delta\phi)$ when performing the template fits. The error bars indicate statistical uncertainties.

The left panel of Fig. 3 shows the $N_{\rm ch}^{\rm rec}$ dependence of v_2 in 13 TeV data for $0.5<p_{\rm T}<5$ GeV and for three different choices of the peripheral multiplicity interval, $N_{\rm ch}^{\rm rec,periph}$: $0 \le N_{\rm ch}^{\rm rec,periph} < 5$, $0 \le N_{\rm ch}^{\rm rec,periph} < 10$ and $0 \le N_{\rm ch}^{\rm rec,periph} < 20$. No clear dependence of the extracted v_2 on the choice of the peripheral interval is observed. One of the assumptions of the template fitting procedure used in this paper is that the v_2 is independent, or weakly dependent, on the multiplicity. Consequently, the template fitting method is devised to account for a v_2 in the peripheral bin (see text of paper near Eq. 5). The independence of the measured v_2 on the choice of the peripheral interval is an independent test of this assumption.

The right panel of Fig. 3 shows the v_2 values obtained when the peripheral pedestal, $Y^{\rm periph}(0)$, is subtracted (i.e. excluded) from $Y^{\rm periph}(\Delta\phi)$ when performing the template fits. This fitting is similar to the peripheral subtraction procedure that has been used in prior ridge analyses in p+Pb collisions, and assumes that there is negligible v_2 in the peripheral interval. Here, the v_2 values obtained depend considerably on the choice of the peripheral multiplicity interval. This difference reflects the bias associated with the "zero yield at minimum" (ZYAM)-subtracted peripheral reference that is discussed in the paper. The bias depends on F and, thus, the choice of peripheral reference. For the 0–5 reference interval for which the bias is smallest, significant v_2 values are observed even in the $5 < N_{\rm ch}^{\rm rec} < 10$ interval indicating non-negligible v_2 even in low-multiplicity events. Thus, the bias with the ZYAM-subtracted peripheral reference discussed in the paper is unavoidable.

A preliminary version of this analysis presented results for the $\Delta\phi$-integrated ridge yield in $\sqrt{s} = 13$ TeV pp collisions. With the observation that the ridge results from a sinusoidal modulation that can be interpreted as a single-particle v_2, there is little physics significance to the ridge yield. However, for completeness and to update the preliminary results, $\Delta\phi$-integrated yields are shown in Fig. 4 for the 13 TeV data. The yields, $Y_{\rm int}^{\rm ZYAM}$, are the traditional measurement of the correlated yields in $Y(\Delta\phi)$ above the ZYAM pedestal and are the results from the preliminary analysis. These yields are severely biased for low $N_{\rm ch}^{\rm rec}$ because the intrinsic shape of the correlation function near $\Delta\phi = 0$ violates the implicit assumptions of the ZYAM method. The quantities $Y_{\rm int}^{\rm a}$ and $Y_{\rm int}^{\rm b}$ represent the yields calculated using the results of the template fitting procedure which properly accounts for the shape of the peripheral correlation near $\Delta\phi = 0$. The yield $Y_{\rm int}^{\rm a}$ is obtained from the correlated component of $Y^{\rm ridge}(\Delta\phi)$ integrated over $|\Delta\phi| < \pi/2$. It is given by $2\pi G\, v_{2,2}$. Alternatively, $Y_{\rm int}^{\rm b}$ represents the correlated yields when including the pedestal of $FY^{\rm periph}(\Delta\phi)$ while calculating the yields. It is given by $2\pi\left[G + FY^{\rm periph}(0)\right] v_{2,2}$. Then, $Y_{\rm int}^{a}$ is the correct yield if all of the pedestal in $Y^{\rm periph}(\Delta\phi)$ is due to hard processes. Thus, it represents a lower bound on the correlated yields. In contrast, $Y_{\rm int}^{\rm b}$ is the correct yield when all of the pedestal in $Y^{\rm periph}(\Delta\phi)$ is due to soft production, and is, therefore, an upper bound on the correlated yields.

Figure 5 shows a comparison of the $v_{2,2}$ obtained from the template fitting prodecure to the $v_{2,2}$ obtained from direct Fourier transform of the $Y(\Delta\phi)$, as a function of $N_{\rm ch}^{\rm rec}$. The difference between the two is largest in lower multiplicity events and decreases with increasing $N_{\rm ch}^{\rm rec}$.

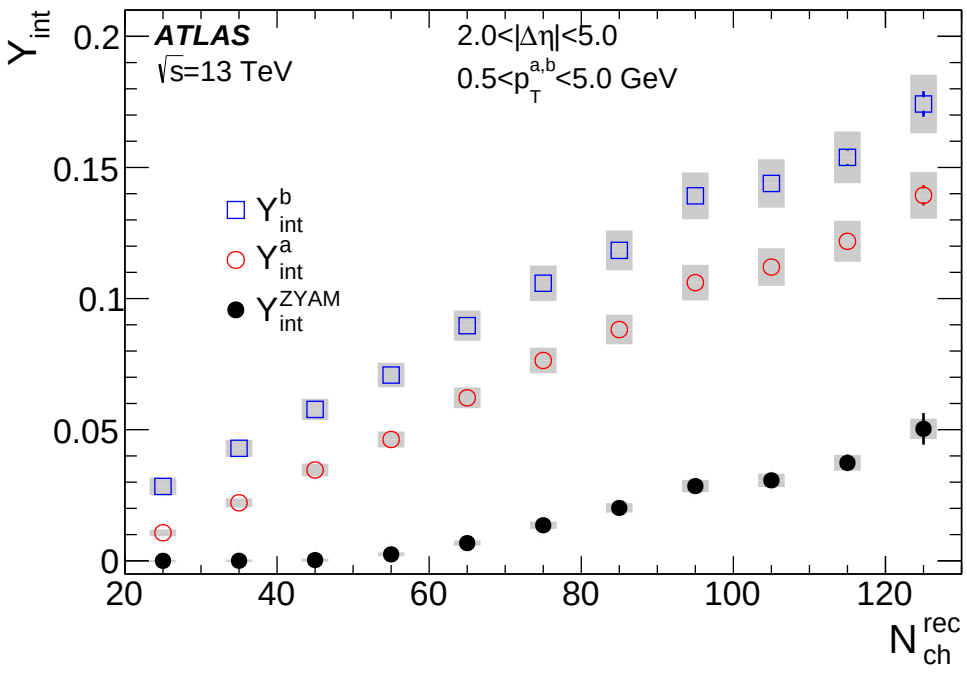

Figure 4: Integrated near-side yields obtained using different procedures (see text) vs $N_{\mathrm{ch}}^{\mathrm{rec}}$ in 13 TeV pp collisions. The vertical error bars and shaded bands indicate statistical and systematic uncertainties respectively.

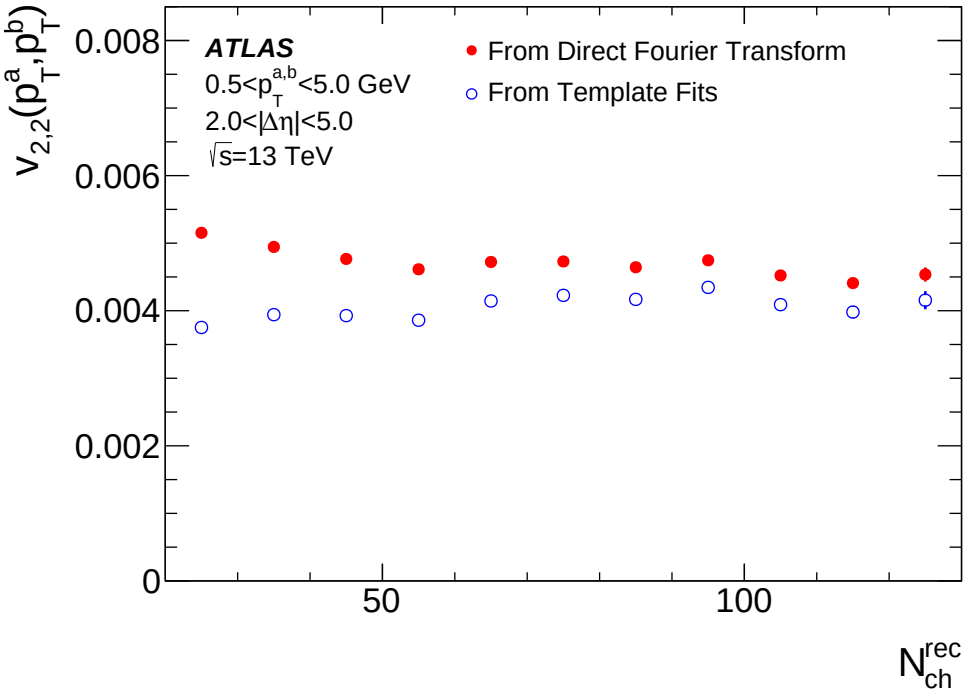

Figure 5: Comparison of the $v_{2,2}$ obtained from the template fitting prodecure to the $v_{2,2}$ obtained from direct Fourier transform of the $Y(\Delta\phi)$, as a function of $N_{\mathrm{ch}}^{\mathrm{rec}}$. The results shown are for 13 TeV pp collisions and for $0.5<p_{\mathrm{T}}^{\mathrm{a,b}}<5.0$ GeV. The error bars indicate statistical uncertainties.